Magnetic anisotropy in Ni–Fe–Ga–Co ferromagnetic shape memory alloys in the single-variant state

2009 J. Phys.: Condens. Matter 21 076001

(http://iopscience.iop.org/0953-8984/21/7/076001)

J. Phys.: Condens. Matter **21** (2009) 076001 (7pp) doi:10.1088/0953-8984/21/7/076001

Magnetic anisotropy in Ni–Fe–Ga–Co ferromagnetic shape memory alloys in the single-variant state

H Morito[1], A Fujita[2], K Oikawa[2], K Fukamichi[1], R Kainuma[1], T Kanomata[3] and K Ishida[2]

[1] Institute of Multidisciplinary Research for Advanced Materials, Tohoku University, Katahira 2-1-1, Sendai 980-8577, Japan
[2] Department of Materials Science, Graduate School of Engineering, Tohoku University, Aoba-yama 6-6-02, Sendai 980-8579, Japan
[3] Faculty of Engineering, Tohoku Gakuin University, 1-13-1 Chuo, Tagajo 980-8537, Japan

E-mail: morito@tagen.tohoku.ac.jp

Received 23 October 2008, in final form 15 December 2008
Published 23 January 2009
Online at stacks.iop.org/JPhysCM/21/076001

Abstract

The effects of the addition of Co on the magnetic anisotropy in $Ni_{55-x}Fe_{18}Ga_{27}Co_x$ ($x = 1$–6) single-variant ferromagnetic shape memory alloys have been investigated. By the addition of Co from 1 to 6 at.%, the Curie temperature T_C is increased from 318 to 405 K, keeping the martensitic transformation temperatures above room temperature. As a result, the value of the uniaxial magnetic anisotropy constant $|K_u|$ at 300 K increases with increasing x of the Co concentration and the martensite phase of $Ni_{49}Fe_{18}Ga_{27}Co_6$ exhibits a relatively high value of $|K_u| = 1.15 \times 10^5$ J m^{-3} at 300 K. With increasing Co concentration, on the other hand, the c axis changes from the magnetic easy axis to the hard axis at 4.2 K, that is, the sign of K_u is reversed from positive to negative between 2 and 3 at.% Co. Furthermore, K_u in $Ni_{53}Fe_{18}Ga_{27}Co_2$ is positive below 100 K and negative above 100 K up to T_C, reducing the magnetic anisotropy around 200 K. From the present results, it is evident that the magnetic anisotropy of $Ni_{55-x}Fe_{18}Ga_{27}Co_x$ ($x = 1$–6) single-variant ferromagnetic shape memory alloys is very sensitive to Co concentration and also temperature.

1. Introduction

In 1996, Ullakko and his co-authors [1] demonstrated that a large strain can be induced by applying magnetic fields to a Ni_2MnGa ferromagnetic shape memory alloy (FSMA) having a thermoelastic martensitic microstructure. After that, FSMA was accepted as a new kind of functional material, combining a large output strain based on characteristics of shape memory alloys with a rapid response comparable to those of conventional magnetostrictive materials. Since demands for actuator materials have been heightened in recent years, the FSMA systems open up new application fields for actuator materials because of their special properties, as well as conventional application fields such as in engineering, communications, medicine, etc. Accordingly, FSMAs have become attractive research topics in the fields of materials science and solid state physics [1–14].

The magnetic-field-induced strain (MFIS) in FSMAs arises from a motion of variant boundaries in the martensite phase [1, 2]. When the martensitic transformation takes place, three possible variants along the crystal axes [100], [010] and [001] are nucleated during the cooling process. In each variant, the magnetic moment is pinned to the magnetic easy axis due to a large magnetic anisotropy. When the magnetic anisotropy energy (MAE) is larger than the driving energy of the variant boundaries, the angle between the magnetization and applied magnetic field direction is lowered by not only the rotation of magnetization but also the variant rearrangement in order that the magnetic easy axis is aligned parallel to the magnetic field direction [1, 2]. As a result, the motions of variant boundaries induce macroscopic strains.

Recently, the Ni_2FeGa alloy has received attention as a new FSMA [15–21]. This alloy undergoes a thermoelastic martensitic transformation from a $B2$ and/or an $L2_1$-Heusler

parent to a martensite phase, following by a seven-layer modulated (14M) structure with a five-layer modulated (10M) structure [15–21]. The Ni_2MnGa alloy with modulated layer structures such as 10M and 14M has a large MAE, accompanied by a large MFIS [1, 2]. On the other hand, the martensite phase of $Ni_{54}Fe_{19}Ga_{27}$ has a large uniaxial magnetic anisotropy constant K_u at low temperatures. However, the value of K_u is not so large in the vicinity of room temperature because of its low Curie temperature T_C [20]. Accordingly, in keeping with the high martensitic transformation temperature, the increase of T_C is essential from a practical viewpoint. In addition, fundamental research of the magnetic anisotropy is important to control the variant orientation efficiently because the MFIS is caused by the variant rearrangement.

Many variants are induced in a self-accommodating manner when the martensitic transformation occurs, and hence the magnetic anisotropy dispersed in the multi-variant state prevents us from evaluating the strict value of the magnetic anisotropy constant. Therefore, the single-variant specimens are necessary for precise measurements. In the present paper, the effects of the addition of Co on the martensitic transformation and the magnetic anisotropy have been investigated for $Ni_{54+x}Fe_{19-x}Ga_{27}$-type alloys in the single-variant state.

2. Experiments

The polycrystalline $Ni_{54}Fe_{19}Ga_{27}$ and $Ni_{55-x}Fe_{18}Ga_{27}Co_x$ ($x = 1$–6) alloys were prepared by arc-melting in an argon gas atmosphere. The single crystals were grown by an optical floating-zone method under a helium gas atmosphere. To prepare the disordered $B2$ phase specimens, these specimens were homogenized at 1433–1473 K for 48 h and quenched in ice water. Subsequently, the specimens were annealed at 673 K for 24 h and cooled in a furnace to obtain the ordered $L2_1$ phase. Note that these alloys have a single-phase structure with β ($L2_1$), although $Ni_{55}Fe_{18}Ga_{27}$ has a two-phase structure with $\beta + \gamma(A1)$.

The powder specimens for x-ray diffraction measurements were ground by using the annealed polycrystalline alloys, and sealing them in a quartz capsule and heat-treating at 1473 K for 15 s and 673 K for 1 h to relieve internal strains in the specimens. The crystal structures of the martensite phase were investigated at 200 K.

The magnetizations were measured with a superconducting quantum interference device (SQUID) magnetometer and also a vibrating sample magnetometer (VSM). The Curie temperature T_C and the martensitic transformation starting temperature T_{Ms} and the finishing temperature T_{Mf}, and the reverse transformation starting temperature T_{As} and the finishing temperature T_{Af}, of the $Ni_{55-x}Fe_{18}Ga_{27}Co_x$ ($x = 3$–6) polycrystalline alloys were determined from the thermomagnetization curves measured in a field of 8 or 40 kA m^{-1} in the heating and cooling process, respectively. In addition, for $Ni_{54}Fe_{19}Ga_{27}$ and $Ni_{55-x}Fe_{18}Ga_{27}Co_x$ ($x = 1$ and 2) alloys, T_C, T_{Ms}, T_{Mf}, T_{As} and T_{Af} were also evaluated from the thermomagnetization curves and differential scanning calorimetry (DSC) measurements, respectively.

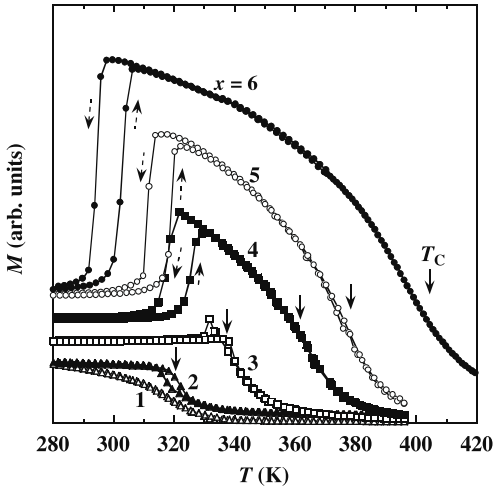

Figure 1. Concentration dependence of the thermomagnetization curves in a magnetic field of 40 kA m^{-1} in the cooling and heating processes for $Ni_{55-x}Fe_{18}Ga_{27}Co_x$ ($x = 1$–6). The dashed arrows indicate the process directions. The solid arrows indicate the Curie temperature T_C.

The crystallographic orientations of the single-crystalline specimens were confirmed by electron backscattering diffraction patterns before heat treatment. The plate-like specimens with the parent phase were trimmed so that the $\langle 100 \rangle_P$, where the subscript P stands for the parent, directions are normal to the faces. In order to obtain the single-variant specimens, uniaxial compressive stresses of about 10–15 MPa were applied to the $[100]_P$ and $[010]_P$ directions in the martensite phase. To confirm the influence of the compressive stress on the formation of variants, the surface of the specimens was observed with an optical microscope. The magnetization curves for the single-variant specimens were also measured up to 4 MA m^{-1} at 4.2–300 K with the SQUID magnetometer. In order to prevent movement during the magnetization measurements, the specimens in the single-variant state were fixed with an adhesive.

3. Results and discussion

Shown in figure 1 are the thermomagnetization curves in a magnetic field of 40 kA m^{-1} for $Ni_{55-x}Fe_{18}Ga_{27}Co_x$ ($x = 1$–6) as a function of the Co concentration in the cooling and heating processes. Figures 2(a) and (b) show the magnetization M and its temperature derivative dM/dT as a function of temperature in a magnetic field of 8 kA m^{-1} in a heating process for $Ni_{54}Fe_{19}Ga_{27}$, respectively. Conventionally, T_C is defined as the minimum temperature of the temperature T dependence of the derivative of the magnetization M curve of dM/dT–T. From figure 2(b), the minimum peak of dM/dT is between 308 and 310 K; therefore the value of T_C for $Ni_{54}Fe_{19}Ga_{27}$ is deduced to be 309 K. To verify the value of T_C, the Arrott plots, M^2 versus H/M [22], were applied to the same alloy as shown in figure 3. The plots were made in 2 K steps in the heating process. By using the linear parts of the $M^2 - H/M$ curves, T_C is determined to be 309 K. The value of T_C obtained from the dM/dT–T curve is in agreement

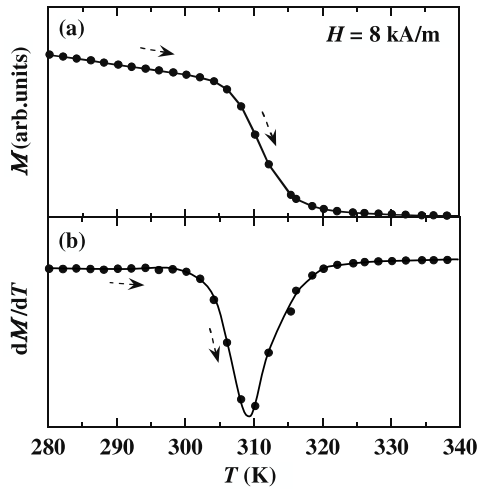

Figure 2. (a) Magnetization M and (b) its temperature derivative dM/dT as a function of temperature in a magnetic field of 8 kA m^{-1} in a heating process for $Ni_{54}Fe_{19}Ga_{27}$.

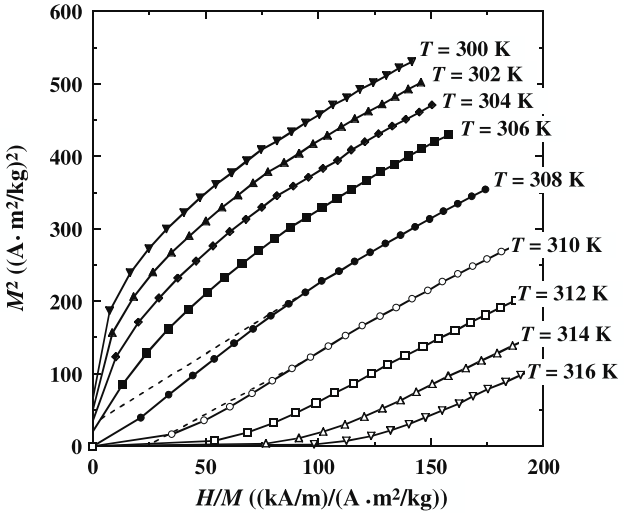

Figure 3. Arrott plots in 2 K steps in the heating process for $Ni_{54}Fe_{19}Ga_{27}$.

with T_C determined from the Arrott plots. In the present study, therefore, T_C of $Ni_{55-x}Fe_{18}Ga_{27}Co_x$ (x = 1–6) is determined from the dM/dT–T curves. In figure 1, the solid arrows indicate the T_C determined by dM/dT.

In the cooling process, there is an increase in magnetization M below T_C and a decrease in M caused by the martensitic transformation in $Ni_{55-x}Fe_{18}Ga_{27}Co_x$ (x = 3–6). On the other hand, the curves of $Ni_{53}Fe_{18}Ga_{27}Co_2$ exhibit a hysteresis around T_C. In the cooling process, the phases in $Ni_{55-x}Fe_{18}Ga_{27}Co_x$ (x = 3–6) change from the paramagnetic parent (PM^P) to the ferromagnetic parent (FM^P), and then to the ferromagnetic martensite (FM^M). Both the paramagnetic to ferromagnetic transition and the martensitic transformation simultaneously take place at the same temperature in $Ni_{53}Fe_{18}Ga_{27}Co_2$. The decrease of M is observed below T_{Ms} because of the change in MAE caused by the martensitic transformation.

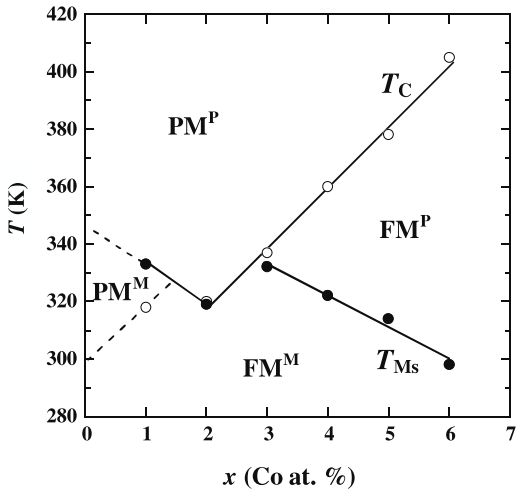

Figure 4. Concentration dependence of the Curie temperature T_C and the martensitic transformation starting temperature T_{Ms} for $Ni_{55-x}Fe_{18}Ga_{27}Co_x$ (x = 1–6). The designations of PM^P, PM^M, FM^P and FM^M stand for the paramagnetic parent, the paramagnetic martensite, the ferromagnetic parent and the ferromagnetic martensite, respectively.

Table 1. The Curie temperature T_C, the martensitic transformation starting temperature T_{Ms} and the finishing temperature T_{Mf}, and the reverse transformation starting temperature T_{As} and the finishing temperature T_{Af}, for $Ni_{55-x}Fe_{18}Ga_{27}Co_x$.

x (at.%)	T_C (K)	T_{Ms} (K)	T_{Mf} (K)	T_{As} (K)	T_{Af} (K)
1	318	333	323	334	343
2	320	319	309	315	325
3	337	332	323	330	337
4	360	322	314	322	328
5	378	314	310	317	321
6	405	298	291	300	306

From the M–T curves in figure 1, T_C, T_{Ms}, T_{Mf}, T_{As} and T_{Af} are determined. The temperatures of T_C, T_{Ms}, T_{Mf}, T_{As} and T_{Af} for the $Ni_{55-x}Fe_{18}Ga_{27}Co_x$ (x = 1–6) polycrystalline alloys are summarized in table 1. The concentration dependences of T_C and T_{Ms} for the $Ni_{55-x}Fe_{18}Ga_{27}Co_x$ (x = 1–6) polycrystalline alloys are given in figure 4. In $Ni_{55-x}Fe_{18}Ga_{27}Co_x$, T_C increases from 337 to 405 K, whereas T_{Ms} decreases from 332 to 298 K with increasing x = 3 to 6. In keeping with the martensitic transformation temperatures above room temperature, T_C is increased by adding Co. As seen from the figure, T_{Ms} is higher than T_C for $Ni_{54}Fe_{18}Ga_{27}Co_1$, and the martensitic transformation occurs around T_C in $Ni_{53}Fe_{18}Ga_{27}Co_2$. Therefore, T_C, T_{Ms}, T_{Mf}, T_{As} and T_{Af} were evaluated from the M–T and DSC curves, respectively. Although T_C linearly increases with increasing x from 2 to 6, T_C of $Ni_{54}Fe_{18}Ga_{27}Co_1$ does not follow the linear tendency because T_C of the martensite phase is higher than that of the parent one, like other FSMAs [10, 11, 16]. Although T_C and T_{Ms} of $Ni_{55}Fe_{18}Ga_{27}$ are not evaluated because it has a two-phase structure with $\beta + \gamma(A1)$, the tendency of the concentration dependence is indicated by the dotted lines in figure 4, expected from data of other FSMAs [10, 11, 16]. The valence electron numbers are assumed to be 10 for Ni, 8 for Fe,

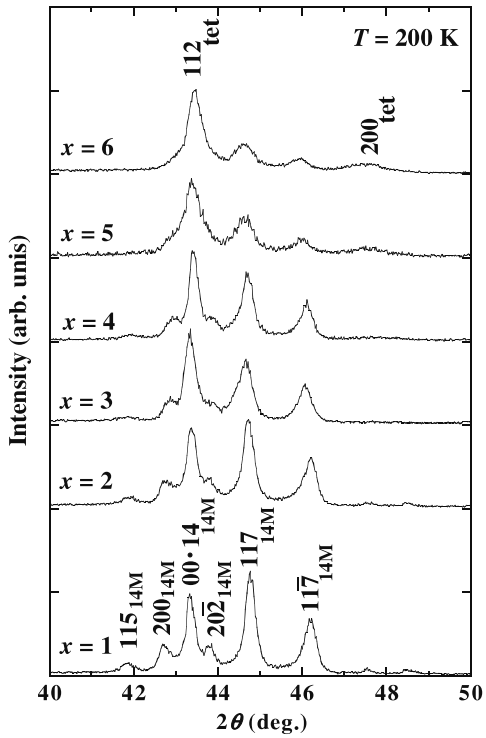

Figure 5. X-ray diffraction patterns at $T = 200$ K for $Ni_{55-x}Fe_{18}Ga_{27}Co_x$ ($x = 1$–6).

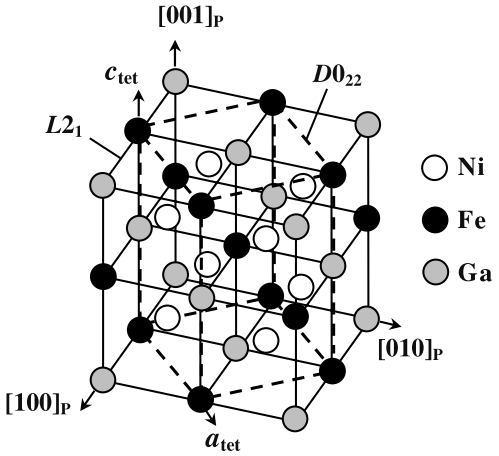

Figure 6. The relation of the crystal structures between the parent and martensite phases in Ni_2FeGa. The solid and dotted lines show the Heusler ($L2_1$) structure of the parent phase and the tetragonal structure ($D0_{22}$) of the martensite phase, respectively.

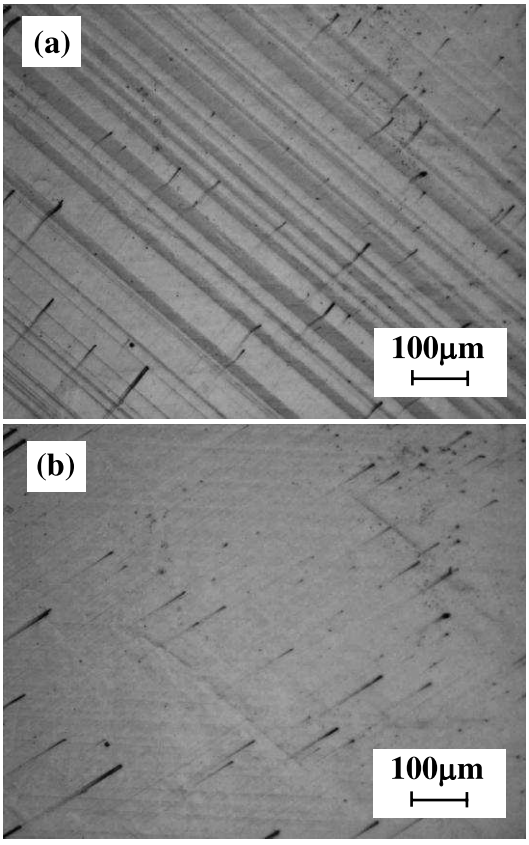

Figure 7. Optical micrographs of the single-crystal $Ni_{49}Fe_{18}Ga_{27}Co_6$ alloy (a) before and (b) after applying compressive stress.

3 for Ga and 9 for Co. Then the value of the valence electron concentration per atom e/a in $Ni_{55-x}Fe_{18}Ga_{27}Co_x$ decreases from 7.72 to 7.69 with increasing Co concentration x from 3 to 6. In ternary Ni_2MnGa and $Ni_{54+x}Fe_{19-x}Ga_{27}$ alloys, T_{Ms} increases with the increase of e/a [23–25]. Therefore, the trend associated with e/a seems also to be applicable in the present $Ni_{55-x}Fe_{18}Ga_{27}Co_x$ alloys. Recently, Kurtulus *et al* have calculated the magnetic exchange interaction between transition elements in full Heusler alloys X_2YZ (X = Co, Ni, Cu, Ph and Pd, Y = Mn, Z = Ga, Si, Ge and Sn) [26]. According to their calculations, T_C is influenced by a strong exchange interaction of the nearest neighbor of X–Y, rather than the interaction of Y–Y. This strongly implies that the magnetic properties, in particular T_C, depend on the nearest-neighbor exchange interaction X–Y. In $Ni_{55-x}Fe_{18}Ga_{27}Co_x$, the Co atoms are considered to occupy the Ni or Fe site. Therefore, the observed increase of T_C in $Ni_{55-x}Fe_{18}Ga_{27}Co_x$ is closely associated with that the Co–Ni and Co–Fe exchange interactions are stronger than the Ni–Fe interaction.

The magnetic-field-induced strain (MFIS) is caused by the reorientation of the martensite variants which are affected by crystal structures. Then, the crystal structures of $Ni_{55-x}Fe_{18}Ga_{27}Co_x$ have been investigated. Figure 5 shows the x-ray diffraction patterns at $T = 200$ K for $Ni_{55-x}Fe_{18}Ga_{27}Co_x$ ($x = 1$–6). For $Ni_{54}Fe_{18}Ga_{27}Co_1$, 115_{14M}, 200_{14M}, $00{\cdot}14_{14M}$, 202_{14M}, 117_{14M}, and $\bar{1}17_{14M}$ peaks defined as the 14M structure are observed. With increasing x, the peak intensities of 115_{14M}, 200_{14M}, 202_{14M}, 117_{14M} and $\bar{1}17_{14M}$ are weak, whereas the 200_{tet} peak associated with the tetragonal ($D0_{22}$) structure, i.e. the 2M structure with no stacking modulation, appears. The intensity of the 200_{tet} peak becomes stronger, showing that the tetragonal structure becomes more stable with increasing x.

When the martensitic transformation occurs, some different variants are induced and such a specimen inevitably becomes in a multi-variant state, preventing us from determining a precise magnetic anisotropy constant because the multi-variant state disperses the magnetic anisotropy in the

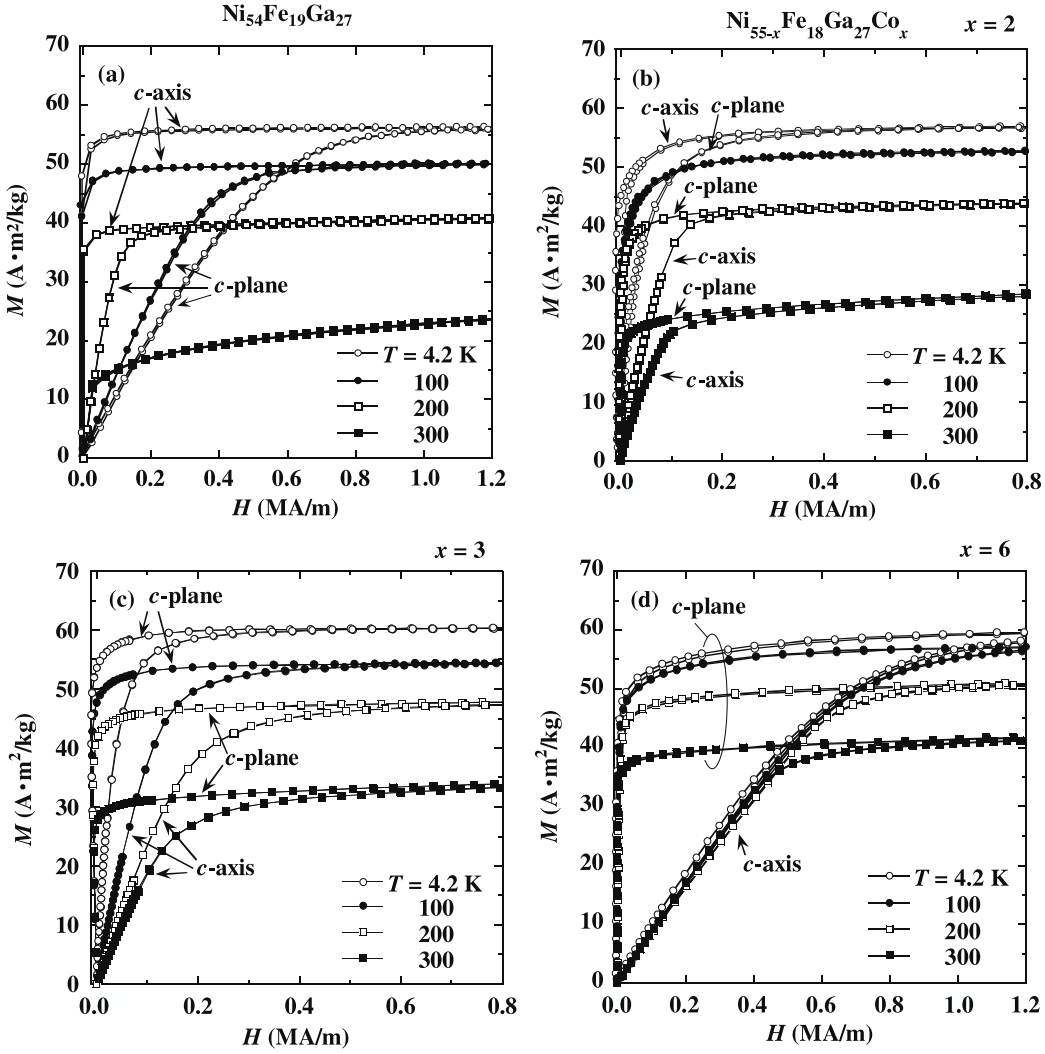

Figure 8. Magnetization curves along the *c*-axis and *c*-plane directions in the single-variant martensite phase for the alloys: (a) $Ni_{54}Fe_{19}Ga_{27}$, (b) $Ni_{53}Fe_{18}Ga_{27}Co_2$, (c) $Ni_{52}Fe_{18}Ga_{27}Co_3$ and (d) $Ni_{49}Fe_{18}Ga_{27}Co_6$.

specimen. Therefore, the single-variant specimen is necessary for detailed investigations. The relation of the crystal structures between the parent and martensite phases in the Ni_2FeGa alloy is illustrated in figure 6. The solid and dotted lines represent the Heusler ($L2_1$) structure of the parent cubic phase and the tetragonal structure ($D0_{22}$) of the martensite phase, respectively. In the former phase, the $\langle 100\rangle_P$ (P: parent) direction corresponds to either the $[110]_M$ (M: martensite) or the c_{tet}-axis direction in the latter phase. In order to obtain the single-variant specimens, uniaxial compressive stresses were applied to the $[100]_P$ and $[010]_P$ directions in the martensite phase. The structures of the $Ni_{55-x}Fe_{18}Ga_{27}Co_x$ ($x = 1$–6) alloys are identified as monoclinic (14M) or tetragonal, depending on x as shown in figure 5. Since a monoclinic structure easily transforms into a tetragonal structure under a low level of applied stress [21], the c_{tet}-axis direction of the tetragonal lattice is oriented in the $[001]_P$ direction by applying compressive stress.

Figure 7 presents the optical micrographs of the surface of the single-crystal $Ni_{54}Fe_{18}Ga_{27}Co_6$ alloy before and after applying compressive stress at room temperature. Various short black lines, like tails of a comet, on the flat surface are extrinsic technical flaws caused by mechanical polishing. Before applying stress as seen from figure 7(a), a clear surface relief pattern is observed, indicating that the martensite phase of the present specimen is in a multi-variant state. After applying stress, the surface relief pattern completely vanishes as shown in figure 7(b). These results indicate that the stress facilitates the growth of specific oriented variants, resulting in a single-variant state.

The uniaxial magnetic anisotropy constant in the single-variant specimens was determined from the magnetization curves measured along the c_{tet} axis ($[001]_P$) and c_{tet} plane ($[100]_P$ or $[010]_P$) of the tetragonal structure. Shown in figure 8 are the magnetization curves (M–H) along the c_{tet} axis and c_{tet} plane as a function of temperature for $Ni_{54}Fe_{19}Ga_{27}$ and $Ni_{55-x}Fe_{18}Ga_{27}Co_x$ ($x = 2$, 3 and 6) in the single-variant state. As illustrated in figure 8(a), the curves of the c_{tet} axis for $Ni_{54}Fe_{19}Ga_{27}$ are easily saturated, whereas the curves for the c_{tet} plane are hardly saturated. These results indicate that the alloy shows a uniaxial magnetic anisotropy, revealing that the c_{tet} axis is the easy axis of magnetization. After correcting the

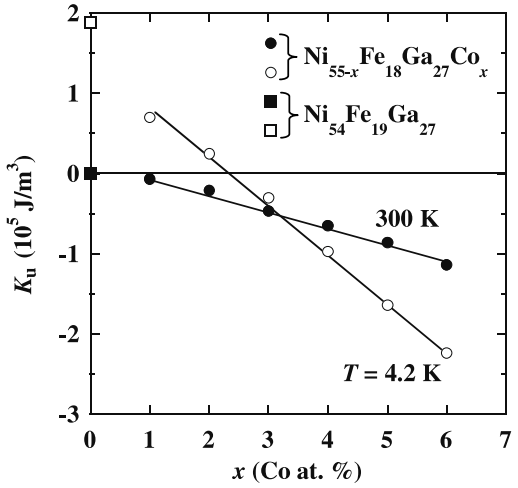

Figure 9. Concentration dependence of the uniaxial magnetic anisotropy constant K_u for the $Ni_{54}Fe_{19}Ga_{27}$ and $Ni_{55-x}Fe_{18}Ga_{27}Co_x$ in the single-variant martensite phase at $T = 4.2$ and 300 K.

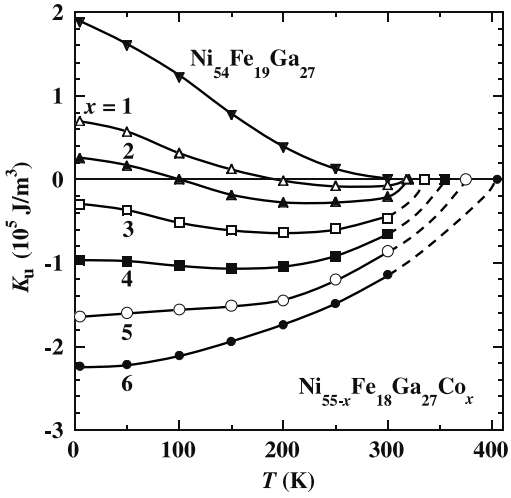

Figure 10. Temperature dependence of the uniaxial magnetic anisotropy constant K_u for $Ni_{54}Fe_{19}Ga_{27}$ and $Ni_{55-x}Fe_{18}Ga_{27}Co_x$ in the single-variant martensite phase.

demagnetizing field, the uniaxial magnetic anisotropy constant K_u is evaluated from the following expression [27]:

$$K_u = \int_0^{M_{sat}} \{H_{hard}(M) - H_{easy}(M)\}\, dM, \qquad (1)$$

where M_{sat} is the saturation magnetization, and H_{hard} and H_{easy} are the magnetic fields applied along the magnetic hard and easy axes, respectively. The area between the magnetization curves along the magnetic easy and hard directions illustrated in figure 8(b) for $Ni_{53}Fe_{18}Ga_{27}Co_2$ is smaller than that for $Ni_{54}Fe_{19}Ga_{27}$, resulting in a smaller MAE. It is interesting to note that both the magnetic easy and hard directions at 4.2 K switch directions at 200 K. The MAE decreases and disappears at 100 K, and reappears above 100 K with increasing temperature. Furthermore, the c_{tet} axis of $Ni_{52}Fe_{18}Ga_{27}Co_3$ becomes the hard axis of magnetization even at 4.2 K as shown in figure 8(c). Namely, the magnetic easy and hard axes of $Ni_{52}Fe_{18}Ga_{27}Co_3$ are opposite to those of $Ni_{54}Fe_{19}Ga_{27}$. The area between the M–H curves along the easy and hard directions increases with temperature and becomes a maximum at $T = 200$ K for $Ni_{52}Fe_{18}Ga_{27}Co_3$. No similar behavior has been observed in other FSMA systems. The c_{tet} axis of $Ni_{49}Fe_{18}Ga_{27}Co_6$ is the hard axis of magnetization as shown in figure 8(d) and MAE decreases with increasing temperature up to T_C.

The concentration dependence of K_u at $T = 4.2$ K and 300 K is given in figure 9 for $Ni_{55-x}Fe_{18}Ga_{27}Co_x$ ($x = 1$–6) and $Ni_{54}Fe_{19}Ga_{27}$ in the single-variant martensite phase. In $Ni_{55-x}Fe_{18}Ga_{27}Co_x$, the value of $|K_u|$ increases from 0.07×10^5 to 1.15×10^5 J m^{-3} with increasing Co concentration from $x = 1$ to 6 at $T = 300$ K. Therefore, the increase of T_C by the substitution of Co effectively increases $|K_u|$ at $T = 300$ K. On the other hand, $Ni_{54}Fe_{19}Ga_{27}$ and $Ni_{55-x}Fe_{18}Ga_{27}Co_x$ ($x = 1$, 2) have a positive value of K_u at $T = 4.2$ K because the c axis is the magnetic easy axis. With increasing Co concentration, the c axis changes from the magnetic easy axis to the hard axis, that is, the sign of K_u is reversed from positive to negative between 2 and 3 at.% Co. Enkovaara *et al* have made theoretical calculations for the MAE within density-functional theory using the full-potential linearized augmented plane-wave method [28]. In their calculations, the generalized gradient approximation was used for the exchange and correlations, and the spin–orbit interaction was treated within the second-order variational method [29]. According to the calculated results, the magnitude of MAE exhibits a broad maximum at $e/a = 30$/f.u. with a lattice distortion of $c/a = 0.94$ in Ni_2MnGa. As a result, the MAE decreases with decreasing e/a. In the case of Ni_2FeGa with $e/a = 31$/f.u., the increase in Co concentration results in the decrease of e/a, accompanied by the increase of $|K_u|$. For more detailed discussion on the relation between the MAE and e/a, the calculations of the MAE for the present alloys are necessary, although the crystal structures of the present alloy system are complicated, depending on the concentration.

The temperature dependence of K_u for $Ni_{55-x}Fe_{18}Ga_{27}Co_x$ and $Ni_{54}Fe_{19}Ga_{27}$ is shown in figure 10, which is different from each other. For example, in the case of $Ni_{53}Fe_{18}Ga_{27}Co_2$, K_u is positive below 100 K and negative above 100 K up to T_C. The saturation magnetization is parallel and perpendicular to the c_{tet} axis below and above 100 K, respectively. Consequently, the temperature where K_u becomes zero is defined as the spin-flop transition temperature T_{sf} which is decreased by the addition of Co.

4. Conclusion

The magnetic properties, in particular the Curie temperature and magnetic anisotropy, have been investigated for $Ni_{55-x}Fe_{18}Ga_{27}Co_x$ ($x = 1$–6). The value of T_C increases with increasing x of the Co concentration, which is accounted for by strong Ni–Co and Co–Fe exchange interactions, compared with the Ni–Fe interaction. The martensitic transformation temperatures of $Ni_{55-x}Fe_{18}Ga_{27}Co_x$ decrease with the decrease of e/a, or the increase of the Co concentration.

By the addition of Co of 6 at.%, T_C is increased up to 405 K, keeping the martensitic transformation temperatures above room temperature. As a results, the single-variant martensite phase in the $Ni_{49}Fe_{18}Ga_{27}Co_6$ exhibits a large value of magnetocrystalline anisotropy constant $|K_u| = 1.15 \times 10^5$ J m^{-3} at 300 K. The magnetic easy and hard axes at 4.2 K are reversed by adding Co, and the c axis of the martensitic phase becomes the magnetic hard axis in $Ni_{49}Fe_{18}Ga_{27}Co_6$. Therefore, the magnetic anisotropy of the $Ni_{55-x}Fe_{18}Ga_{27}Co_x$ ($x = 1$–6) single-variant ferromagnetic shape memory alloys is very sensitive to the Co concentration and also temperature. In addition, the spin-flop temperature T_{sf}, defined as the temperature where K_u becomes zero, decreases with increasing x in $Ni_{55-x}Fe_{18}Ga_{27}Co_x$ ($x = 1$–2).

Acknowledgments

The authors wish to thank Messrs T Ota and T Takagi for their experimental support. A part of the present study was supported by the Ministry of Education, Culture, Sports Science and Technology, Japan, and by the Grant-in-Aids for Scientific Research, Core Research for Evolutional Science and Technology (CREST) and the Research Fellowship of the Japan Society.

References

[1] Ullakko K, Huang J K, Kantner C, O'Handley R C and Kokorin V V 1996 *Appl. Phys. Lett.* **69** 1966
[2] O'Handley R C 1998 *J. Appl. Phys.* **83** 3263
[3] Heczko O, Sozinov A and Ullakko K 2000 *IEEE Trans. Magn.* **36** 3266
[4] Murray S J, Marioni M, Allen S M, O'Handley R C and Lograsso T A 2000 *Appl. Phys. Lett.* **77** 886
[5] Sozinov A, Likhachev A A, Lanska N and Ullakko K 2002 *Appl. Phys. Lett.* **80** 1746
[6] Sozinov A, Likhachev A A and Ullakko K 2002 *IEEE Trans. Magn.* **38** 2814
[7] James R D and Wuttig M 1998 *Phil. Mag.* A **77** 1273
[8] Kakeshita T, Takeuchi T, Fukuda T, Tsujiguchi M, Saburi T, Oshima R and Muto S 2000 *Appl. Phys. Lett.* **77** 1502
[9] Fujita A, Fukamichi K, Gejima F, Kainuma R and Ishida K 2000 *Appl. Phys. Lett.* **77** 3054
[10] Oikawa K, Wulff L, Iijima T, Gejima F, Ohmori T, Fujita A, Fukamichi K, Kainuma R and Ishida K 2001 *Appl. Phys. Lett.* **79** 3290
[11] Oikawa K, Ota T, Gejima F, Ohmori T, Kainuma R and Ishida K 2001 *Mater. Trans.* **42** 2472
[12] Morito H, Fujita A, Fukamichi K, Kainuma R, Ishida K and Oikawa K 2002 *Appl. Phys. Lett.* **81** 1657
[13] Wuttig M, Li J and Craciunescu C 2001 *Scr. Mater.* **44** 2393
[14] Craciunescu C, Kishi Y, Lograsso T A and Wuttig M 2002 *Scr. Mater.* **47** 285
[15] Oikawa K, Ota T, Sutou Y, Ohmori T, Kainuma R and Ishida K 2002 *Mater. Trans.* **43** 2360
[16] Oikawa K, Ota T, Ohmori T, Tanaka Y, Morito H, Fujita A, Kainuma R, Fukamichi K and Ishida K 2002 *Appl. Phys. Lett.* **81** 5201
[17] Liu Z H, Zhang M, Cui Y T, Zhou Y Q, Wang W H, Wu G H, Zhang X X and Xiao G 2003 *Appl. Phys. Lett.* **82** 424
[18] Morito H, Fujita A, Fukamichi K, Ota T, Kainuma R, Ishida K and Oikawa K 2003 *Mater. Trans.* **44** 661
[19] Murakami Y, Shindo D, Oikawa K, Kainuma R and Ishida K 2003 *Appl. Phys. Lett.* **82** 3695
[20] Morito H, Fujita A, Fukamichi K, Kainuma R, Ishida K and Oikawa K 2003 *Appl. Phys. Lett.* **83** 4993
[21] Sutou Y, Kamiya N, Omori T, Kainuma R, Ishida K and Oikawa K 2004 *Appl. Phys. Lett.* **84** 1275
[22] Arrott A 1957 *Phys. Rev.* **108** 1394
[23] Chernenko V A 1999 *Scr. Mater.* **40** 523
[24] Tsuchiya K, Ohashi A, Ohtoyo D, Nakayama H, Umemoto M and McCormick P G 2000 *Mater. Trans.* **41** 938
[25] Oikawa K, Ohmori T, Sutou Y, Morito H, Kainuma R and Ishida K 2007 *Metall. Mater. Trans.* **38** A767
[26] Kurtulus Y, Dronskowski R, Samolyuk G D and Antropov V P 2005 *Phys. Rev.* B **71** 014425
[27] O'Handley R C 2000 *Modern Magnetic Materials* (New York: Wiley) p 181
[28] Enkovaara J, Ayuela A, Nordstrom L and Nieminen R M 2002 *Phys. Rev.* B **65** 134422
[29] MacDonald A H, Pickett W E and Koelling D D 1980 *J. Phys. C: Solid State Phys.* **13** 2675